Dehydration and reduction reactions favored under medium pressure and temperature assisted by photocatalysis

A. Flory, F. Dappozze, C. Guillard

Catalytic transformation under medium pressure and temperature assisted by photocatalysis in presence of TiO_2

Arthur Flory, Frederic Dappozze, Chantal Guillard

University Lyon, University Claude Bernard, CNRS, IRCELYON, UMR5256, Villeurbanne 69626 (France)

*chantal.guillard@ircelyon.univ-lyon1.fr

Abstract

The impact of UV irradiation on the catalytic transformation of dihydroxyacetone molecule (DHA) has been investigated under inert atmosphere, medium pressure (5 Bars) and temperature (<=120°C) in presence of commercial anatase TiO_2 samples (UV100 and A100), rutile TiO_2 (R100) and mixture of anatase and rutile phase (P90). In absence of light, the main products formed are pyruvaldehyde and lactic acid whatever the temperature playing only a role on kinetic. Under UV irradiation, we highlighted their decomposition and the formation of new compounds, hydroxyacetone (HydA) in high concentration and acrylic acid (AcrAc) together with H_2, CO_2 and acetaldehyde in gas phase and new condensation products. The higher the number of photons emitted, the greater the HydA and AcrAc formation highlighting the importance of light and especially of the (e^-, h^+) pairs generated by photocatalysis. Actually, whereas the formation of HydA and AcrAc is similar in presence of all TiO_2 samples containing anatase phase, these compounds are formed in low concentration in presence of TiO_2 rutile. Mechanisms of the formation of hydA and AcrAc under photocatalysis assisted by pressure and temperature were discussed considering the formation of H^+ and reducing agent made possible thanks to simultaneous oxidation reaction occurring via h^+ and or OH°

Keywords:

Photocatalysis, DHA, TiO_2, hydrogen, hydroxyacetone, reduction

1- Introduction

Biomass represents one of the largest sources of carbon in nature and is part of the range of renewable sources contributing to a carbon-free energy mix. With the aim of valorizing biomass and thus limiting the use of fossil energy, hydrothermal catalysis under inert gas is commonly used in various industrial applications, such as the production of hydrogen and the conversion of biomass into chemicals generally in presence of catalysts based on noble metals such as platinum (Pt), palladium (Pd), rhodium (Rh) and ruthenium (Ru) deposited on solid supports, such as oxides (TiO_2 , Al_2O_3, ZrO_2,...) to improve their stability and dispersion [1, 2]. In addition to the use of noble metals, high temperatures and pressures are used, which makes the process very energy-intensive and expensive. On the other hand, several reviews on the conversion of biomass by photocatalysis show that this process may be interesting for converting biomass into a compound of interest. [3-7]. This process has the advantage of working at room temperature and atmospheric pressure with metal oxides as catalyst and in particular TiO_2 with, as in the previous case, a noble metal, the most effective being Pt or less expensive metals such as Cu. However, the conversion efficiency of this method is still quite low compared with catalytic hydrothermal processes [8]. Recently, there has been significant research on the influence of temperature on photocatalysis. Some of these publications deal with energy to form H_2 using plasmonic thermophotocatalysis [9] or hydrogenation reaction such as Fisher-Tropsch reaction in

presence of strontium titanate and cobalt [10, 11] but most studies in this area focus on depollution of water or air generally in the presence of catalyst based on TiO_2 [12, 13

] or $SrTiO_3$ [14-16] in all cases in presence of a metal (Pt or Ag) and in the range of temperature from 60°C to 240°C. Additionally, other catalysts such as g-C_3N_4, ZnO [17] or a manganese-based catalyst such as MnOx-TiO_2 [18] or Mn_3O_4/$MnCO_3$ [19]. These studies collectively demonstrate enhanced photocatalytic degradation of these compounds at temperatures ranging from 60°C to 150°C and even up to 240°C. A recent review [20] on Photo-/thermal synergies in heterogeneous catalysis conclude that photo-thermo synergies are complex and fundamental interpretation is still at a rudimentary level and most of the studies do not identify the dominant physico-chemical mechanisms governing the reactions. Despite this work on photo-thermo catalysis, there is limited research on the integration of photocatalysis and hydrothermal processes. A few publications have explored this area and main are focused on CO_2 reduction for example working at 190°C under autogene pressure in the presence of Ag/ g-C_3N_4under visible light [21], or in the presence of Au/TiO_2 up to 95°C and 20 bar [22-24]. Additionally, three other publications have delved into this topic, shedding light on the synergistic effects between photocatalysis and hydrothermal processes for energy production. For example, an enhancement of hydrothermal gasification of glucose due to the photocatalytic action of TiO_2, led to the formation of H_2 and CH_4 under conditions of 30 MPa and 350−450°C [25]. An improvement in H_2 production during acid hydrolysis of cellulose in the presence of photocatalysis and Pt/TiO_2 is also observed [26] and recently our publication on valorization of glucose [27].

While a synergistic effect is confirmed by coupling photocatalysis and hydrothermal processes, the mechanisms remain to be further investigated. Is this due to the generation of Bronsted acid by photocatalysis favoring hydrothermal reactions as suggested in our previous publication. [27]. Or is it due to the Lewis acid sites present on TiO_2 and their increase under UV irradiation? Indeed, under UV irradiation of TiO_2, electron-hole pairs are formed on the surface of TiO_2, thus improving its Lewis acid character and making it more capable of accepting electron pairs from Lewis bases. Or, is the impact of light on hydrothermal process due to another phenomenon?

In order to deep the mechanisms involved in this process coupling we focused on the conversion of dihydroxyacetone, a crucial molecule for assessing catalyst acidity. Indeed, initially, dihydroxyacetone is transformed into pyruvaldehyde by dehydration in the presence of Bronsted acid. Pyruvaldehyde then converts to lactic acid in the presence of strong Lewis acid site. Firstly, we will compare the disappearance of dihydroxyacetone and the products resulting from its transformation under hydrothermal conditions in the presence of different TiO2 whose acid-base properties are known [28] then we will study the impact of UV irradiation. All experiments will be carried out under argon inert gas.

2- Materials and methods

2.1. Materials

All the compounds used were analytical reagents and used without further purification. Dihydroxyacetone (DHA), Lactic acid (LA), pyruvaldehyde (PA), glyceraldhyde (GA), Fructose (Fru), Glucose (Glu), Levulinic Acid (Lev Ac), acetone (Ac), hydroxyacetone (hydr Ac), pentane-dione (Pent Di), lactide (Lact), 5-Hydroxymethylfurfural (5-HMF), 2-furoic acid (2-FurA) were supplied by Sigma Aldrich, Merk and Thermo Scientific or Across Organics as standard for hydrothermal process assisted or not by photocatalysis.. Milli-Q water ($18M\Omega.cm^{-1}$) was used throughout the whole experiments.

Four commercial titanium dioxide were used. Two pure TiO2 anatase Hombikat UV100 purchased from Sachtleben Chemie (Duisburg, Germany) and HPX-200/v2 (named A100) from Cristal, one mixte TiO_2 anatase and rutile TiO2 P90 (80% anatase, 20% rutile) from Evonik, and a pure TiO2 rutile phase HPX-400C (named R100) from Cristal. Their characteristics are given in Table 1

Catalyst	UV100	A100	P90	R100
Surface area (m^2/g)	300	96	115	85
Acid sites density ($\mu mol.m^{-2}$) [28]	3	2.9	3.5	4.8
Basic sites density ($\mu mol.m^{-2}$) [28]	0.4	0.2	0.13	1
Acid/Base sites ratio [28]	7.5	13.7	27	4.8

Table 1: Surface area, acid site, basic site and acid/Base sites ratio of TiO2 UV100, A100, P90 and R100

Ultrapure water (18 MΩ) and methanol (*Semiconductor Grade,* 99.9% pure) from Alfa were used as solvents for all the syntheses and analyses.

2.2. Dihydroxyacetone transformation

DHA transformation was assessed by hydrothermal process assisted or not by photocatalysis. The reactor is a stainless-steel autoclave of 100 mL equipped with a sapphire window in its bottom allowing to work under irradiation, temperature and pressure. The reactor is described in our previous publication [27]. All reactions were conducted in the presence of 0.5 g/L of DHA aqueous solution, and of TiO_2 catalyst under 5 bar of argon. The mixture was mechanically stirred at 500 rpm. Only temperature and irradiation varied: i) hydrothermal reactions were conducted at 90°C or 120°C without irradiation, ii) photocatalytic reactions were conducted at ambient temperature and under UV irradiation (PLL-lamp: 18 W, 365 nm and 6.2 mW/cm²) and iii) hydrothermal reactions assisted by photocatalysis were conducted at 120 °C and under the same UV irradiation than photocatalytic reactions. The reactions begin in the following manner: initially, water and TiO_2 are placed within the autoclave and heated to the reaction temperature. Subsequently, the appropriate amount of DHA is introduced. If required, UV irradiation is initiated immediately, marking the starting point of the reaction. 500 µL were sampled at different time and filtrated on MILLEX HVLP 0.45 µm hydrophilic filter (Millipore) prior to HPLC analysis.

DHA conversion (%) and products yields (%C) are calculated as follows:

Conversion (%) = (DHA consumed) / (initial DHA)*100

Product i Yield (%C) = (Product i molar concentration)/(DHA initial molar concentration)*(Product i carbon number)/3*100

Analytical procedure

High-Performance Liquid Chromatography (HPLC)

The dihydroxyacetone and the products formed in aqueous phase, were quantified by HPLC Shimadzu Prominence system equipped with a refractive index detector (RID), a photometric diode array detector (PDAD).

The dihydroxyacetone and the products formed were analyzed through an ultrafast high-performance liquid chromatography (HPLC) (Shimadzu SPD-M20A) assembled with a Transgenomic ICSep ICE-COREGEL-87H3 organic acid column. 277 µL/L of H2SO4 served as the mobile phase at a flow rate of 0.7 mL min-1 and the temperature of the oven was 30 oC. The nature and concentration of the products of DHA transformation were determined using RID and PDAD at 210 nm the UV detector at the wavelength of 210 nm. The identification of the products involved injecting standard aqueous solutions alongside the products resulting from the transformation of DHA, and then verifying their UV spectra by deconvolution.

HPLC/MS analysis

HPLC/MS analysis was also done by using UPLC (U3000, Thermo Fisher Scientific) UPLC chain (U3000, Thermo Fisher Scientific) coupled to a high-resolution hybrid quadrupole-time-of-flight mass spectrometer (Impact II, Bruker). For the separation a column: Macherey-Nagel – Nucleodur C18 HTec EC250/4.6 5µm and a mobile phase 85% water / 15% Methanol at a flow rate of 1000 µL/min was used. Mass spectrometry detection was done by electrospray in positive mode (ESI +)

Gas phase analysis

Gaseous products were analyzed using gas chromatograph (Clarus 590 : Perkin Elmer) directly connected to the reactor. Lighter compounds (H_2, Ar, O_2, N_2, CH_4, CO) were separated with a RT-Msieve5A molecular sieve type column (30m x 0.32mm x 30µm df - Restek) whereas the other products were separated using a PoraPlot Q column (25m x 0.53mm x 20µm df - Agilent J&W Technologies), then oxidize into CO_2 before reducing them to CH_4 through a Polyarc (R) system (Activated Research Company) and detected with a flame ionization detector (FID).

3- Results and discussion

3.1. Transformation DHA under mild pressure and temperature

3.1.1. Impact of the nature of TiO_2

The impact of the presence of different TiO_2 (anatase, rutile and mixture of anatase rutile) on the degradation of DHA under 120°C and 5 Bars of argon was represented Fig.1. Pure rutile R100 and pure anatase UV100 led to the most rapid transformation of DHA whereas the anatase/rutile mixture (P90) is similar to A100 (pure anatase TiO_2). These results are relatively similar to those already obtained in our previous publication using high concentration of DHA (10g/L) and catalyst (10g/L) except for rutile samples which only lead to a slight improvement of the transformation of DHA compared to UV100. This different behavior may be due to the low concentration of DHA, 20 times lower, used in this work leading to a modification of the interaction between the catalyst and the DHA.

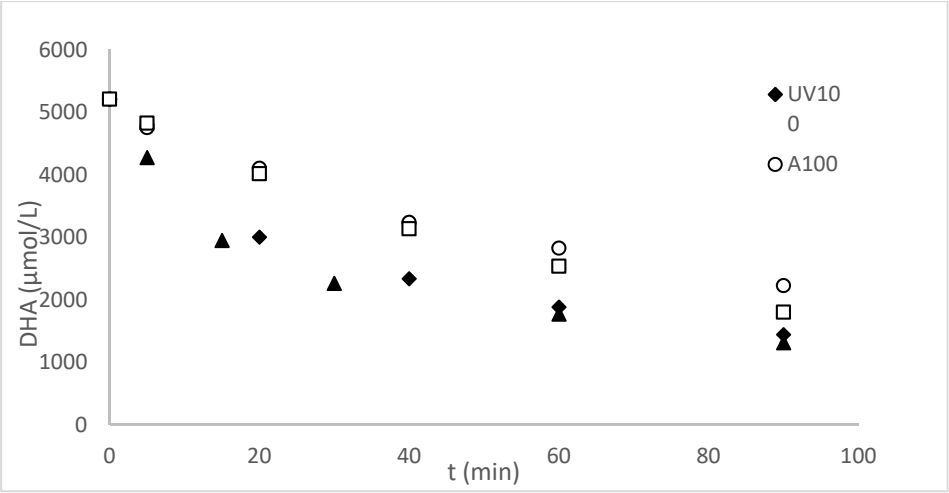

Figure 1: Disappearance rate of DHA in presence of different commercial TiO2 (anatase phase (UV100 and A100), rutile phase (R100) and mixture of anatase and rutile (P90) under 120°C and 5 Bar.

In all cases, under 120°C and 5 Bar, DHA was mainly transformed into pyruvaldehyde (PA) and lactic acid (LA). PA issue from the dehydration of DHA is converted into lactic acid in presence of Lewis acid site [29, 30] Their evolution presented in Fig. 2 shows that PA was more slowly converted into lactic acid (LA) on rutile than on UV100 and on P90 and A100. This behavior already observed in our previous publication using concentrations of DHA and catalysts 20 times more important has been explained considering acid/base balance of the TiO_2 samples. The higher basic sites density present in rutile phase (R100) leads also to the formation of glyceraldehyde, glucose and fructose [28]. Actually, in presence of R100, glyceraldehyde, glucose and fructose are formed in a more important concentration compared to those detected with TiO_2 containing anatase phase. The evolutions of glyceraldehyde, glucose and fructose under 120°C, 5 Bars are given in Fig. S1. However, opposite to our previous work obtained using 10g/L of DHA and catalyst, fructose, issue from aldol condensation of DHA and glyceraldehyde due to basic site, [31,32] is not the main product formed in presence of rutile phase although its formation is more important with rutile phase compared to anatase phase.

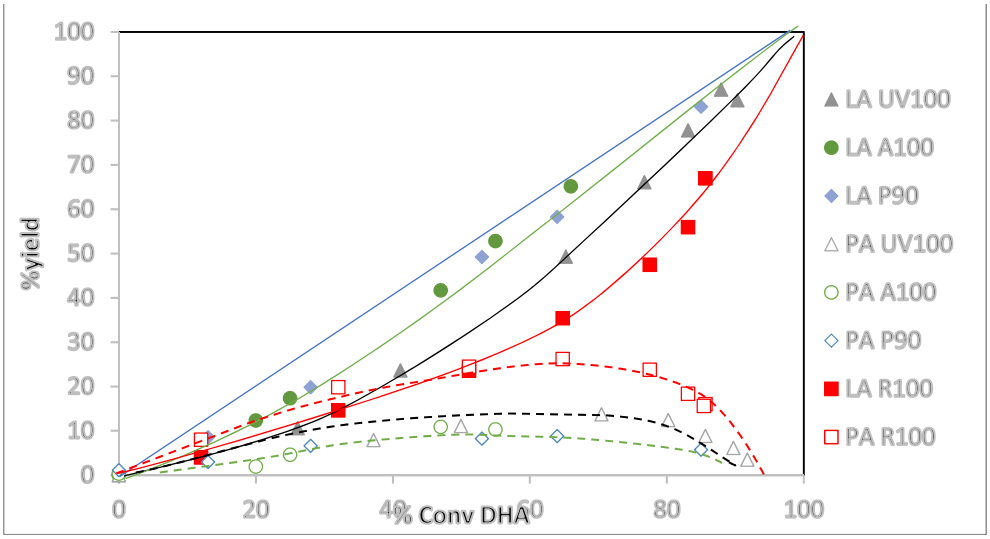

Figure 2: Yield of pyruvaldehyde and lactic acid as a function of DHA conversion. In presence of TiO2 UV100 and A100 (pure anatase phase), TiO2 P90 (80%Anatase, 20% Rutile) and TiO2 R100 (pure rutile phase)

Some condensation products are also observed at high retention time using COREGEL-87H3 organic acid column. Two of these products has been identified as $C_6H_6O_3$ using other conditions (C18 column). These compounds have the same formula than 2,5 HMF which is mentioned in literature as a product of dehydration of fructofuranose isomer [33]. However, these products have not the same retention time than 2,5-HMF. As fructose can have different isomer forms such as α- or β-fructofuranose (**the five-member ring form of fructose)** or α- or β- fructopyranose (**the six-member ring form of fructose)**. We suggest that in our case the products $C_6H_6O_3$ formed could come from the dehydration of the six-member ring form of fructose given pyran cycle (2-hydroxymethyl-pyran-4-one or 4-hydroxy 2H-pyran 2-carbaldehyde or 3- hydroxy 2H-pyran 2-carbaldehyde**) (Scheme 1a).**

Another, possibility for explaining $C_6H_6O_3$ formula could be the dimerization of pyruvaldehyde as described in publication of H.E. Krizner [34] (Scheme 1b)

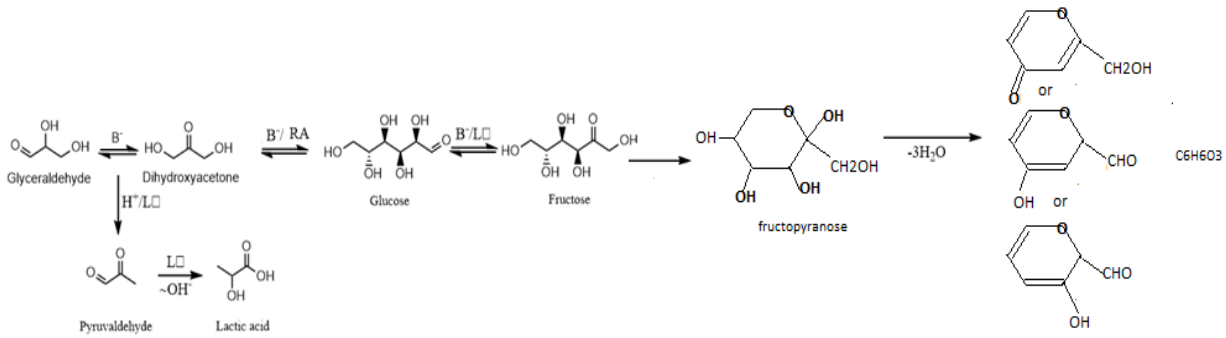

(a)

Or

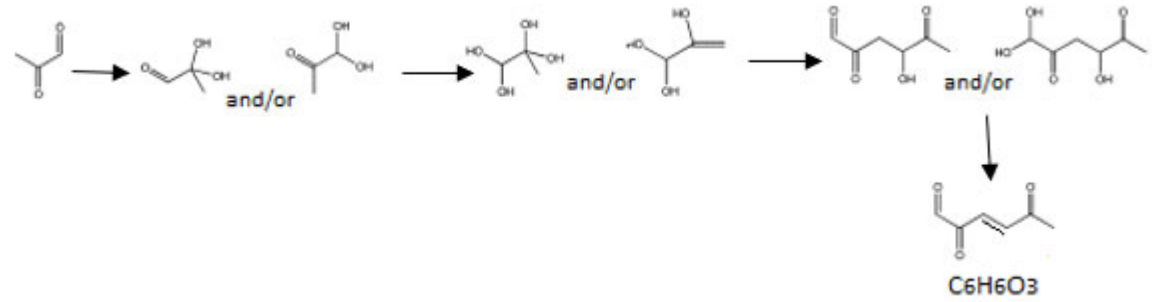

(b)

Scheme 1: transformation of DHA under 120°C, 5 Bar in presence of TiO_2 UV100 from fructopyranose (a) and oligomerization of pyruvaldehyde

3.1.2. Impact of the temperature

Transformation of DHA was performed under two temperatures, 90°C and 120°C and a pressure of 5 bar using only TiO_2 UV100. By increasing temperature, DHA transformation is improved. At 90°C, after 3h a conversion of 37% was obtained against 90% at 120°C (Fig. 3).

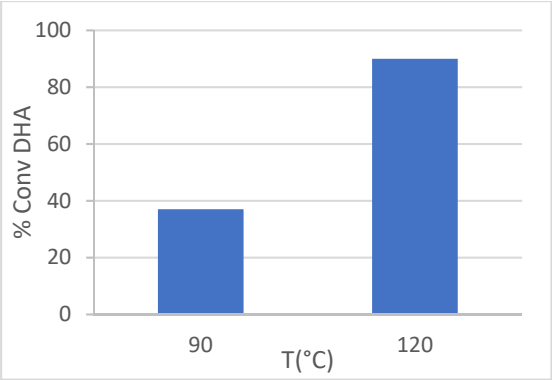

Figure 3: DHA conversion as a function of temperature in presence of TiO2 UV100

In both cases the two main products formed are pyruvaldehyde (PA) and lactic acid (LA); coming from the dehydration of DHA followed by the conversion of pyruvaldehyde into lactic acid in presence of Lewis acid site as described in several publications [29, 30]. Temperature only impact the kinetic of the reaction and not mechanism as observed in Fig. 4 representing the yield of LA and Pyruvaldehyde as a function of DHA conversion.

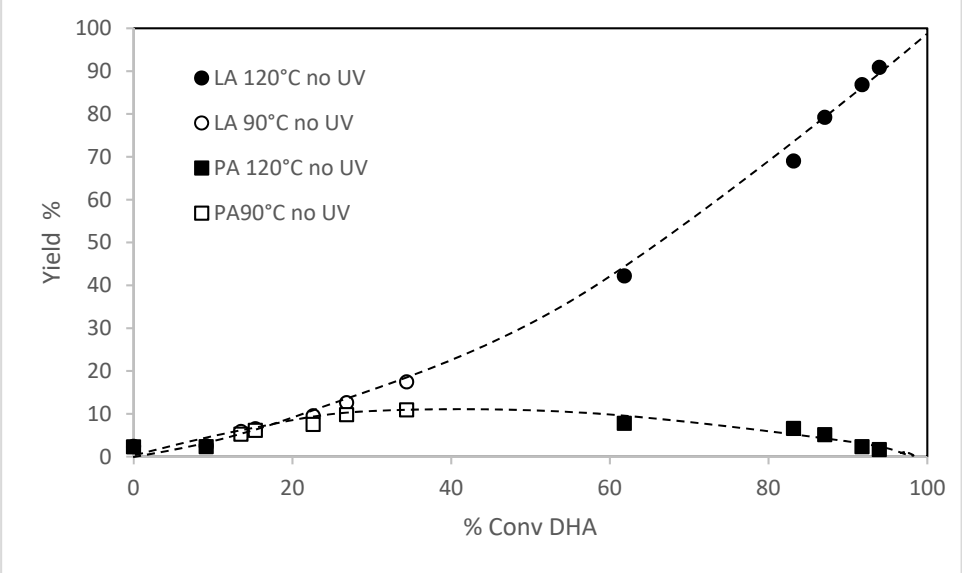

Figure 4: Yield of Lactic Acid (LA) and Pyruvaldehyde (PYR) as a function of DHA conversion in presence of TiO2 UV100 at 90°C (empty symbol) and 120°C (full symbol)

3.2. Impact UV on DHA transformation under pressure and temperature

3.2.1. Impact UV on DHA conversion at ambient temperature, 90°C and 120°C in presence of TiO2 UV100

First, the impact of UV on DHA transformation in inert atmosphere at 5 Bar using **TiO2 UV100** has been compared at different temperatures, ambient temperature (pure photocatalysis), 90°C and 120°C. DHA transformation are given in Figure 5.

Whereas, negligible conversion was obtained under photocatalysis due to a rapid recombination of (e^-, h+) pairs in absence of scavenger of electron, DHA transformation under mild pressure and temperature allowed a rapid conversion of DHA which seems to be slightly decreased under UV light irradiation. Similar observation has already been observed in our previous publication on glucose

transformation [27]. This slight decrease of DHA degradation in presence of combined process could be explained by the variation of the electronic properties of the TiO_2 surface under UV-irradiation ($Ti^{4+} \rightarrow Ti^{3+}$; $O^{2-} \rightarrow O^{\circ -}$) or by the recombination of e-/h+ which can modify the thermodynamic equilibrium at the semiconductor surface due to the heat generated as observed by calculation of adsorption constant in the dark and under light [35-37]

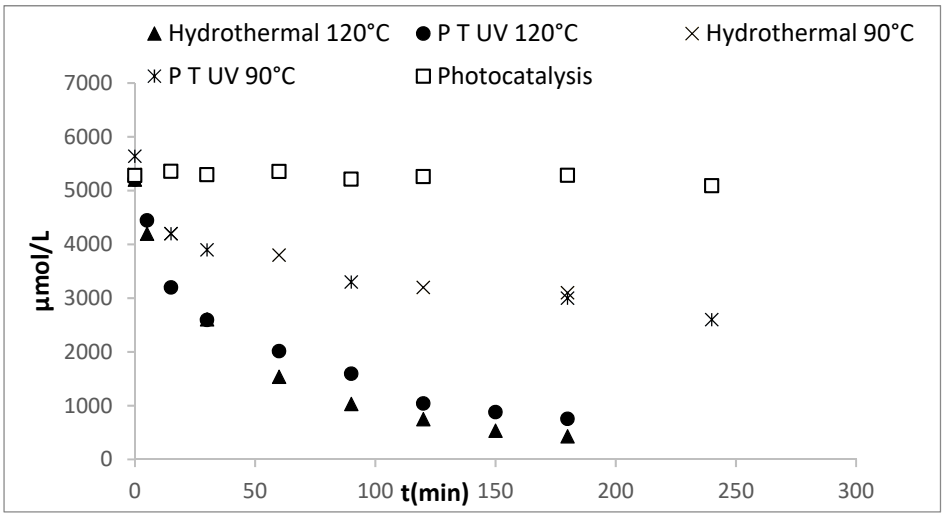

Figure 5 : DHA transformation in inert gas as a function of reaction time in presence of TiO_2 UV100 either under photocatalysis (5.5 mW/cm^2); hydrothermal process (90°C , 5 bar or 120°C, 5 bar) and hydrothermal process assisted by photocatalysis (P T UV: 90°C , 5 bar or 120°C, 5 bar, UV:5.5 mW/cm^2)

3.2.2. Impact of UV on products formed under pressure (5 Bar) and temperature (120°C) in presence of TiO2 UV100

Even if combined process has only small impact on DHA conversion compared to individual processes, whatever the temperature (90°C or 120°C), the formation of the two main products, LA and PA, decrease in presence of UV (Fig.6) and the decrease is favored by increasing the irradiance (Fig.6b). By increasing the temperature from 90°C to 120°C, we also observed an increase of the formation of new products.

Under UV, at 120°C the transformation of PA and LA is clearly observed (Fig. 5b) showing that the greater the irradiance, the more the transformation of LA and PA occur. After about 50% of DHA conversion under 5.5 mW/cm^2 of UV, PA is transformed especially at high irradiation (5.5 mW/cm2) and we can clearly observed the degradation of LA which begin only after a DHA conversion of about 80% under a lower irradiance of 2.2 mW/cm^2.

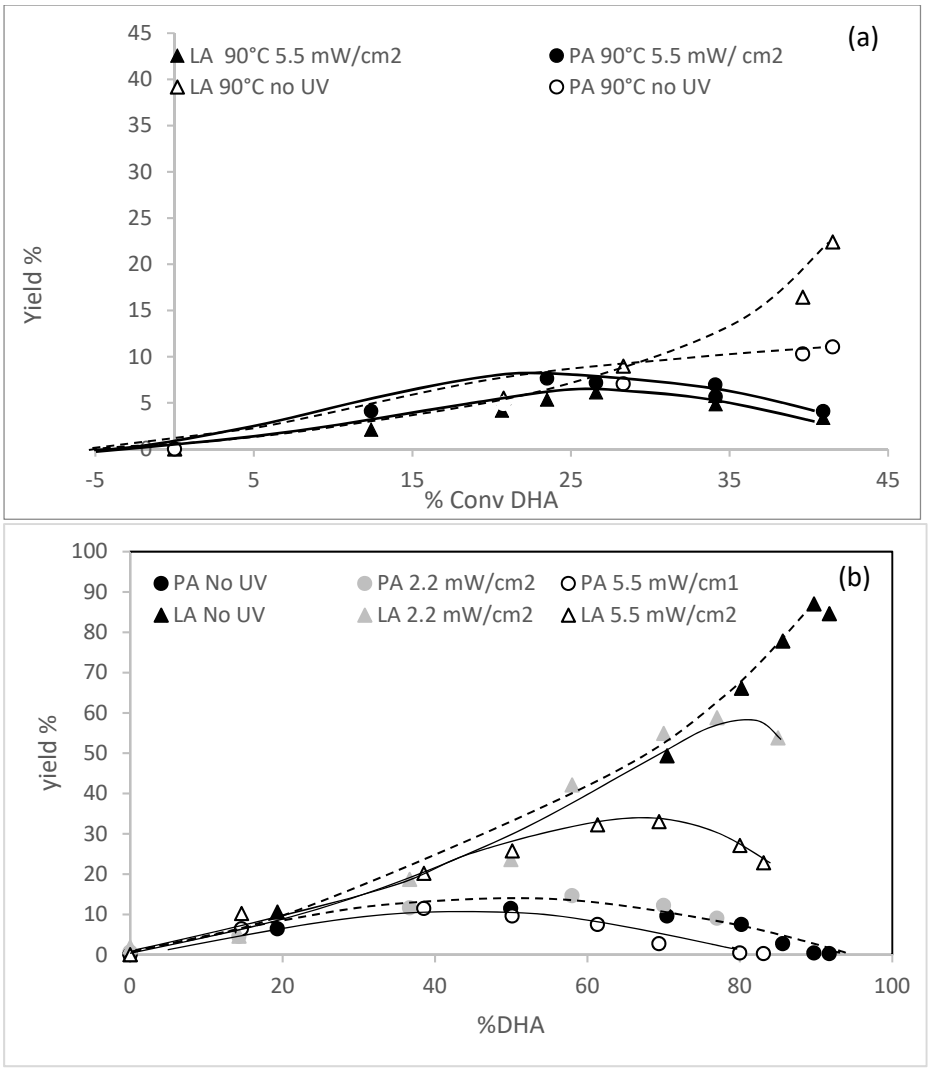

Figure 6: Yield of LA and PA as a function DHA conversion in presence of TiO_2 UV100 without UV and with 5.5 mW/cm^2 UV-A at 90°C (a) and at 120°C under 2.2 mW/cm^2 and 5.5 mW/cm^2 UV-A (b).

Under pure photocatalysis (ambiant temperature), negligeable photocatalytic degradation of DHA under inert atmosphere is observed. Moreover, the photocatalytic transformation of PA and LA used as initial product is also negligeable suggesting that the transformation of PA and LA observed under photocatalysis assisted by temperature and pressure is probably due to their reaction with some species generated during irradiation of TiO_2 favoring their transformation or the modification of TiO_2 surface state.

Similar behavior of UV was observed on the formation of glyceraldehyde (GA) (Fig. S2) but also on fructose and glucose.

Several new products are also observed in presence of UV under hydrothermal conditions, using TiO_2 UV100, especially at 120°C and under 5.5 mW/cm2.

Chromatogram obtained with RI detector (Fig. 7a) and PDA detector at 210nm (Fig.7b) in presence of TiO_2 UV100 after 180 min of reaction under 120°C, 5 Bar with (PTUV) and without UV (PT).

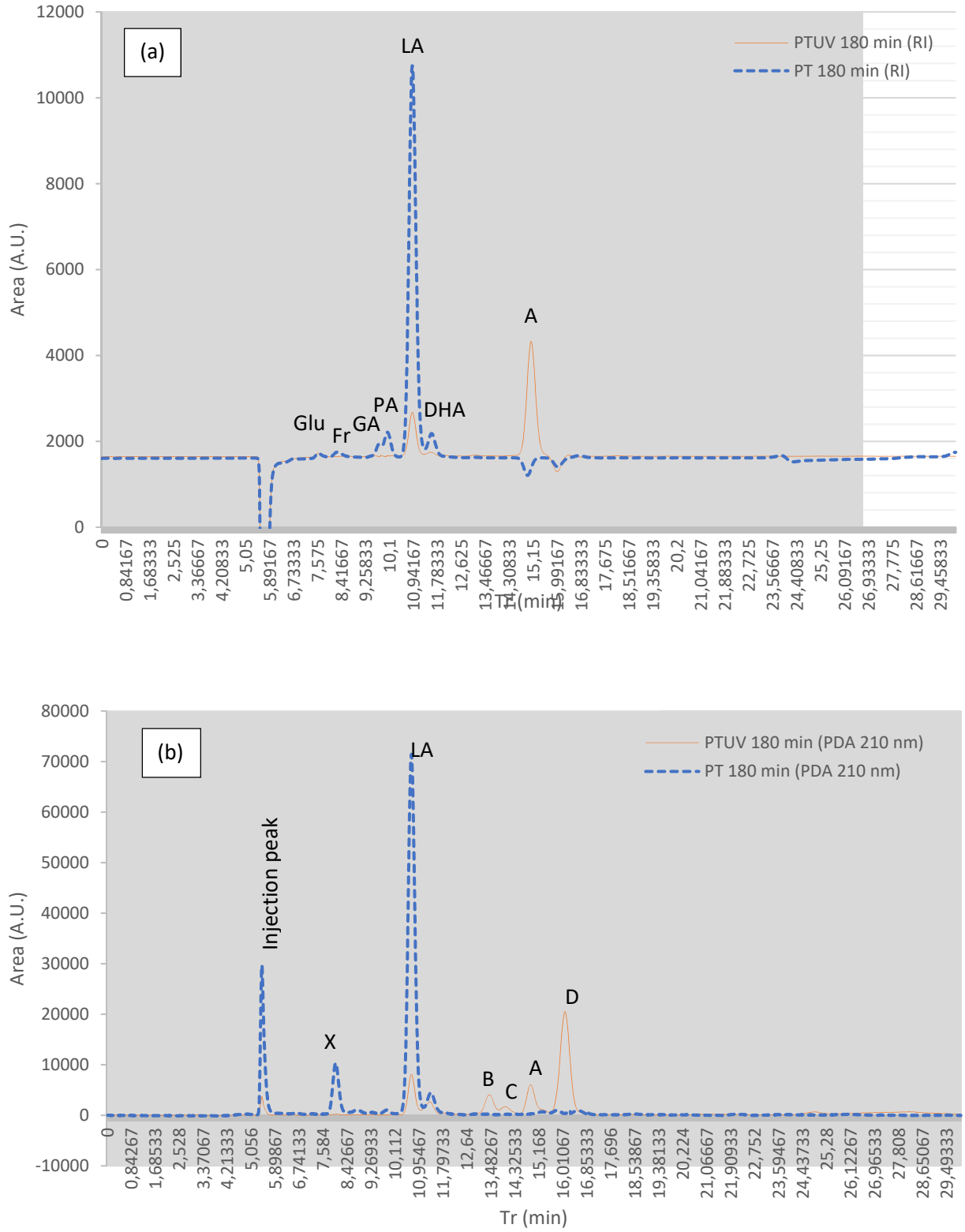

Figure 7 : Chromatogram obtained with with RI detector (a) and diode array detector at 210 nm (b) after 180 min of reaction under PT (120°C, 5 Bar) and PTUV (120°C, 5 Bar and UV-A) in presence of TiO2 UV100

Beside the impact of photocatalysis on the transformation of PA, LA and GA formed at 120°C and 5 Bar, new products are formed.

One new compounds is clearly observed with RI detection (Compounds A in Fig 7a) whereas four new compounds are detected by PDA at 210 nm. Compound A, already detected by RI, and three other componds.

Compound A has a retention time close to that of levulinic acid (LevAc) but it has not the same UV spectrum. Moreover, a coelution of solution obtained after 180min PTUV with a standard solution of levulinic acid (LevAc) showed a spliting of the peak in both types of detector (RI or PDA) confirming that this compound is not levulinic acid. This compound A was attributed to Hydroxyacetone due to the same retention time and UV spectrum. Moreover, a perfect coelution between these two solution confirms that hydroxyacetone is formed.

Compound D has been identified as acrylic acid compound also using standard solution and coelution.

Unfortunately, the two other compounds, B and C have not been identified. These two unknown products do not correspond to acetone, pentane-dione or lactide issue from condensation and esterification. Due to their UV spectrum fig. S3., the two other compounds have probably several aldehyde and/or ketone groups.

We also observed under 120°C and 5 Bar (PT),the compound X with PDA detector at 210 nm. This product **X** cannot be neither fructose or glucose due to its UV spectrum (a shift of UV absorption from 190 nm to 210 nm was observed). This product has been identified as pyruvic acid (Pyr Ac). Methylglyoxal is a reactive α-dicarbonyl compound which easily transformed into pyruvic acid by the addition of a water molecule across the C=O double bond even in the absence of oxygen. Pyruvic acid is completely degraded after 180 min under coupling process PTUV in presence of TiO_2 UV100.

Other products observed with PDA detector at 265 nm (small signal situated at high retention time 33.2 min, 34.9 min ; 38.6 min et 42.3 min) have also been detected only under hydrothermal process assisted by photocatalysis. Without UV, only one compound was observed at high retention time (Tr=36.6 min).

To try to identify some of these compounds we also used C18 column with MeOH/water as eluant to be able to perform HPLC/MS. The overlay of chromatograms obtained after 180 min of reaction in presence of TiO2 UV100 under 120°C and 5 bar in blue and 120°C, 5 bar, 5 mW/cm2) in red, is given in Fig.S4.

The peaks situated near 6.5 and 9.5 min obtained mainly in absence of UV correspond to $C_6H_6O_3$ whereas the peaks observed at 7.1min and 15.5min under UV in presence of PTUV are respectively $C_5H_6O_2$ and $C_6H_8O_2$. The MS of these three peaks are given in Fig. S5. Their formation shows that condensation products are also formed in agreement with litterature under hydrothermal process. However, as explained in paragraph 3.1, $C_6H_6O_3$ does not correspond to 2,5-HMF issue from the dehydration of the five-member ring form of fructose but probably to a similar chemical pathways of dehydration of the six-member ring form of fructose or to dimerisation of PA.

Under photocatalysis assisted by pressure and temperature, we also highlight the formation of H2, CO2 and acetaldehyde not observed or only in small amount using individual processes.(Fig. 8)

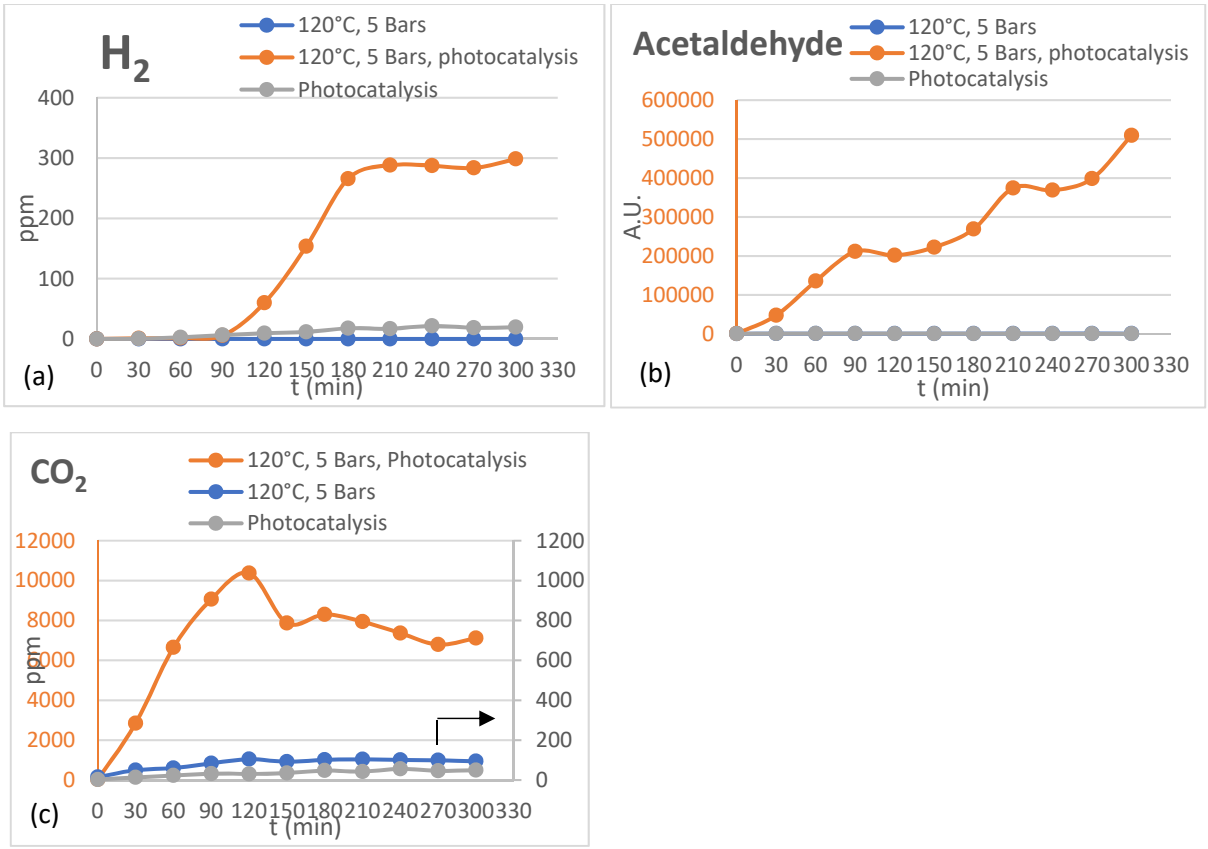

Figure 8: Formation of H_2 (a), (CO) and acetaldehyde during the transformation of DHA under photocatalysis (5.5 mW/cm2):, temperature and pressure (120°C, 5 Bars) and coupling process (PTUV: 110°C, 5 Bars and 5.5 mW/cm2) using TiO2 UV100. *Remarks*: CO and acetaldehyde have not been quantified

3.2.3. Impact of TiO_2 nature on the evolution of product formed under pressure, temperature and UV

Under only photocatalysis in inert atmosphere, whatever the TiO_2, transformation of DHA is negligible. Moreover, for all photocatalyst DHA transformation observed under pressure and temperature is no or only slightly decreased in presence of photocatalysis.

However, as previously observed with TiO_2 UV100, in presence of A100 and P90, containing anatase phase, an important impact of photocatalysis on the formation of PA, LA, Pyr Ac and GA issue from hydrothermal process was observed. Photocatalysis promotes their degradation but also the formation of acrylic acid and hydroxy-acetone, both compounds not observed in absence of irradiation (Fig.9). In the opposite, in presence of TiO_2 rutile, the impact of photocatalysis on PA, LA and GA degradation is low (Fig.S6) and only a small amount of acrylic acid and hydroxy-acetone are formed (Fig.9). However, both B and C compounds observed only under PTUV, are formed in similar amount in presence of rutile or anatase phase.

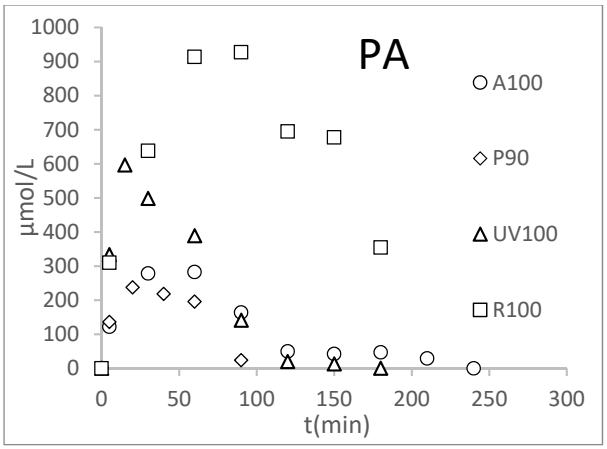
PA
µmol/L
t(min)
A100
P90
UV100
R100

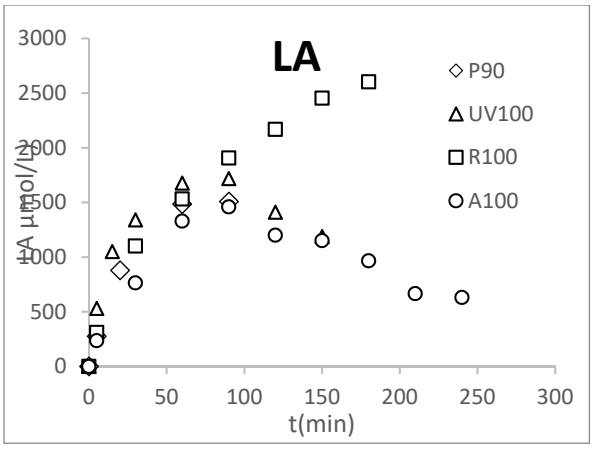
LA
µmol/L
t(min)
P90
UV100
R100
A100

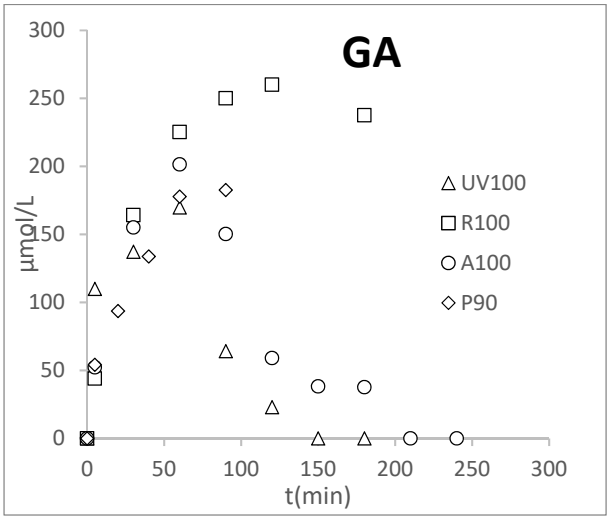
GA
µmol/L
t(min)
UV100
R100
A100
P90

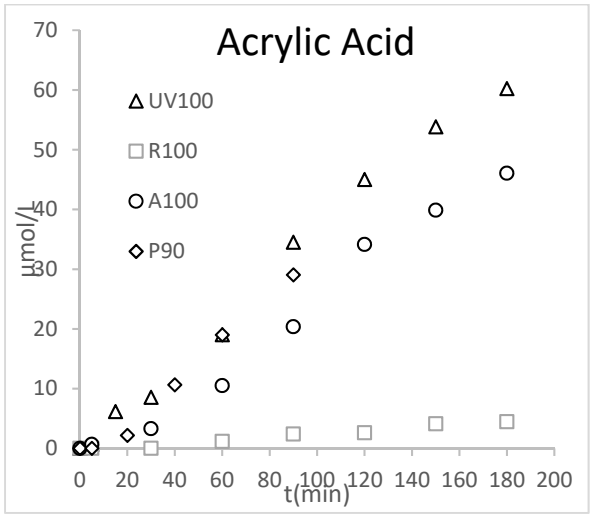
Acrylic Acid
µmol/L
t(min)
UV100
R100
A100
P90

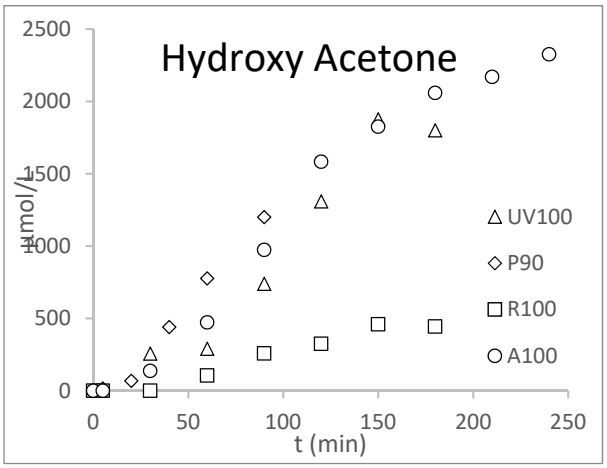
Hydroxy Acetone
µmol/L
t (min)
UV100
P90
R100
A100

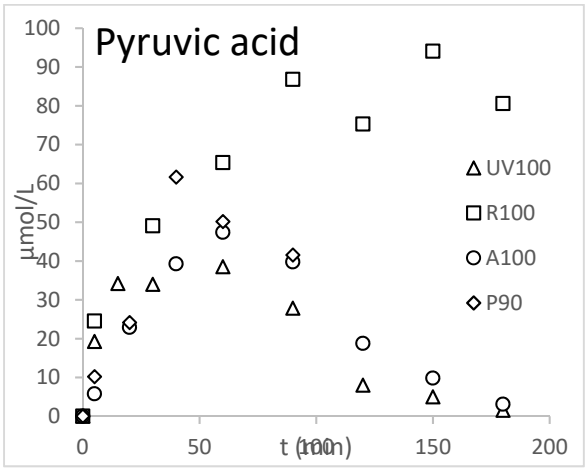
Pyruvic acid
µmol/L
t (min)
UV100
R100
A100
P90

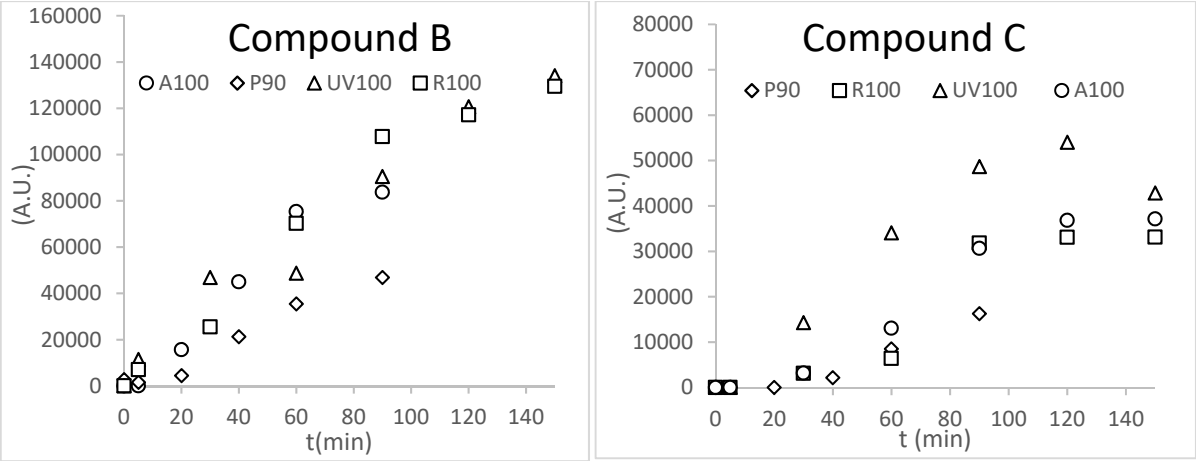

Fig.9: Formation of pyruvaldehyde (PA), lactic acid (LA), Pyruvic acid (Pyr Ac), glyceraldehyde (GA), acrylic acid, hydroxyacetone and unknown products (B, C) in presence of UV100, A100, R100 and P90 under 120°C 5 bar and UVA

3.2.4. Proposition of reactional pathways of DHA transformation under photocatalysis assisted by pressure and temperature.

Whatever the TiO_2 used, an UV irradiation favors the transformation of PA and LA, the products issue from hydrothermal process, together with the formation of hydroxyacetone and acrylic acid. However, we observed that the greater the impact of UV (case of TiO_2 containing an anatase phase), the more hydroxyacetone and acrylic acid are formed. This behavior suggests that the both new compounds come from the transformation of PA and LA. To prove that we performed the degradation of PA (Fig.10a) and LA (Fig. 10b). Their transformation in presence of TiO_2 UV100, 120°C and 5 bar confirm that hydroxyacetone is formed from PA (Fig.10a) and that acrylic acid come from the transformation of LA (Fig. 10b).

During the transformation of PA, in addition of the LA and hydroxyacetone formation, we also observed the formation of pyruvic acid. Moreover, if we compare the amount of acrylic acid formed from LA and from PA, we highlight its more important formation from PA, about50 µmol/L compared to 8µmol/L from LA suggesting that some compounds or species formed during PA favor acrylic acid formation.

No formation of hydroxyacetone and acrylic acid was detected with individual process, photocatalysis or hydrothermal process of PA or LA.

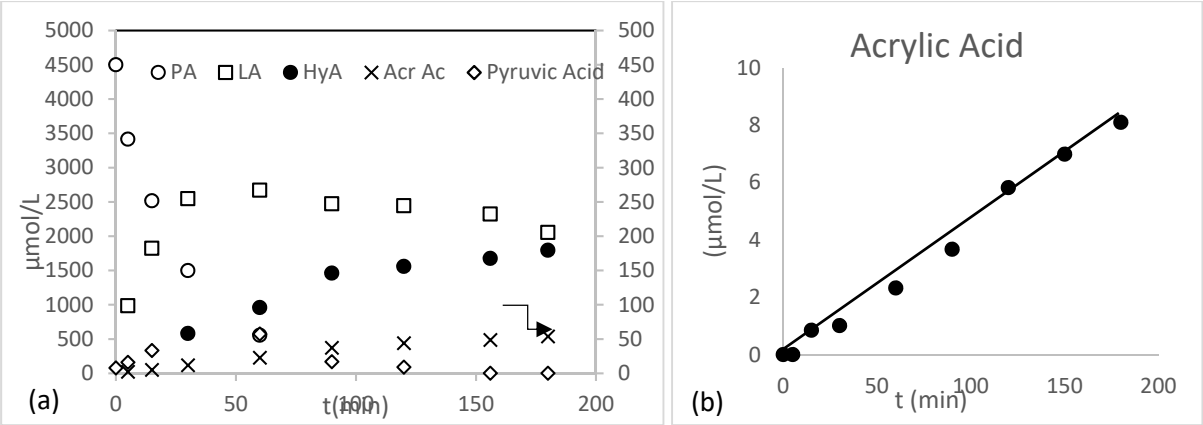

Figure 10: (a) Transformation of pyruvaldehyde (PA) as a function of time under hydrothermal process assisted by photocatalysis in presence of TiO_2 UV100, (b) formation of acrylic acid as a function of time under 5 bar, 120°C and 5.5 mW/cm^2 during the decomposition of 0.5/L lactic acid in inert gas in presence of TiO2 UV100

In literature, hydroxyacetone can be formed from PA by different pathways:

-Pathway 1: dimer formation of PA and electrocyclic opening [38]. Electrocyclic ring opening are initiated by the application of heat or light energy to the cyclic compound, which promotes the movement of electrons within the molecule.

- Pathway 2: cross Cannizzaro reaction between PA and formaldehyde or an aldehyde with no alpha hydrogens [39]. The Cross-Cannizzaro reaction requires the presence of a strong base, usually sodium hydroxide (NaOH) or potassium hydroxide (KOH).

- Pathway 3: a reducing agent such as H2 generated by photocatalysis [40] or another reducing agent.

In our case, reaction path 1 seems unlikely due to the greater formation of PA in the presence of rutile TiO_2 which should favor its dimerization and light irradiation should improve the opening of the ring. Which is not the case, the concentration of hydroxy-acetone is more important in presence of TiO_2 containing anatase phase. On the other hand, for the second reaction paths strong basic conditions and formaldehyde or aldehyde are necessary. These types of aldehyde have not been observed but cannot be exclude due to the presence of unknown peaks B and C. Moreover, are hydroxyl ions generated by auto-protolysis of water enough for this cross Cannizzaro reaction?

So, we suggest that the formation of hydroxyacetone could be due to either:

- the simultaneous oxido-reduction reaction of PA thank to (e^-, h^+) pairs generated by photocatalysis and (H^+, OH^-) formed by protolysis of water under temperature and pressure. The presence of (e^-, h^+) pairs and (H^+, OH^-) simultaneously on TiO_2 surface favors their reaction and the generation of OH° and H°. These radicals could easily react with PA, a reactive α-dicarbonyl compound formed on the surface of TiO_2 from DHA. A simultaneous oxydation of one molecule of PA with OH°and reduction of another molecule of PA would happen.The simultaneous reactions which could occur are resumed in equations [1 - 6].

$2e^- + 2H^+ \rightarrow 2H°$ Equation 1

$2h^+ + 2OH^- \rightarrow 2OH°$ Equation 2

OH° + CH_3-CO-COH $\rightarrow\rightarrow$ CH_3-CO-COOH + H° Equation 3

CH_3-CO-COOH + **OH°**→ CH_3-CO° + **CO_2** + H_2O Equation 4

CH_3-CO° + H° → **CH_3COH** Equation 5

CH_3-CO-COH + **2 H° (or H_2)**→ **CH_3-CO-CH_2OH** Equation 6

This first proposition is resume in the box of Scheme2

Or

-the reduction of PA directly by electron and then H^+, or indirectly by generation of H_2 formed under pressure, temperature and UV. This reduction will be favored due to electronic modification of TiO_2 surface generated (e-, h+) favoring the adsorption of LA on TiO_2 surface and its subsequent oxidation improving the charge separation and the reaction of electron directly on PA, or indirectly through the generation of H_2 to form hydroxyacetone.

H_2 can be formed through DHA transformation into HCO-CO-CH_2OH and HCO-CO-COH which could be the both B, C unknown products or through transformation of LA into pyruvic acid and H_2. Formation of H_2 is presented in Fig. 8 a

Pyruvic acid can react with h^+ to form acetaldehyde and favored electron generation by increasing charge separation (Scheme 2).

In this both propositions of mechanism to form hydroxyacetone, acetaldehyde and CO_2 are generated and experimentally observed (Fig. .8 b, c)

Formation of acrylic acid is explained considering the generation of H^+ by photocatalysis issue from reaction of h^+ with H_2O or with organic compounds such as carboxylic acid and alcohol favoring dehydration of lactic acid.

A proposition of DHA mechanism under hydrothermal process assisted by photocatalysis is given in Scheme 2

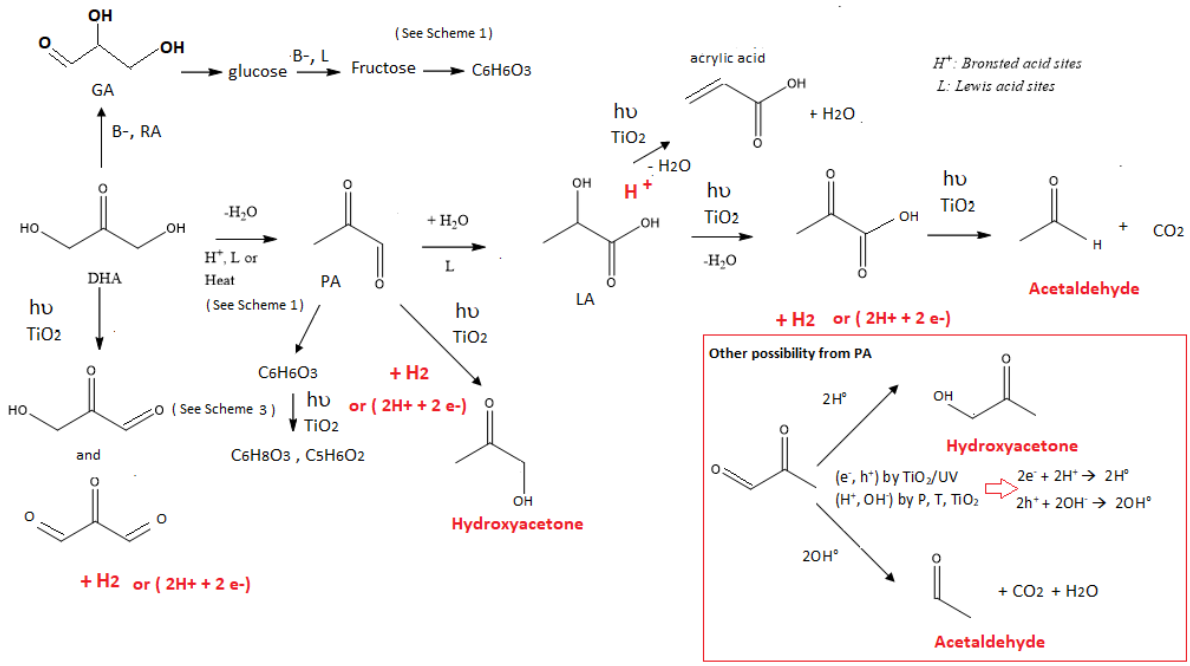

Scheme 2: Proposition DHA mechanism under hydrothermal process assisted by photocatalysis

Besides the new formation hydroxyacetone and acrylic acid in presence of hydrothermal process assisted by photocatalysis, we also observed the formation of the two products $C_6H_8O_3$ and $C_5H_6O_2$ under PTUV conditions. Their formation can be explained by transformation of $C_6H_6O_3$ coming from fructose (scheme 3a) or dimerization of PA (Scheme 3b). The mechanism previously proposed to explain the formation of hydroxyacetone is also adapted to the formation of these two products (Scheme 3a). $C_6H_8O_3$ can also be explained following Scheme 3 b

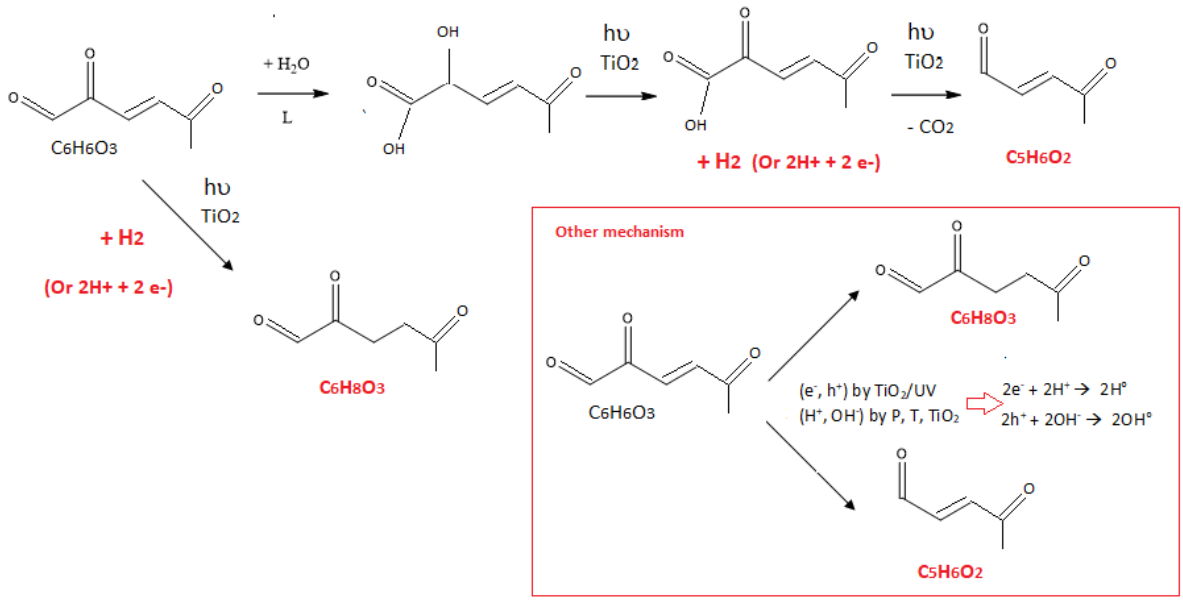

(a)

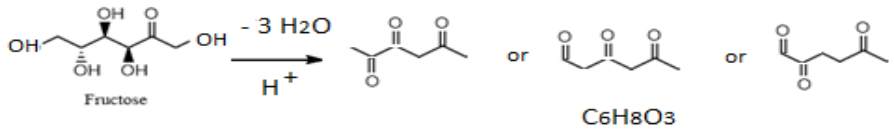

(b)

Scheme 3a, b: Chemical pathway of $C_6H_8O_3$ and $C_5H_6O_2$ formation under PTUV

4. Conclusion:

The transformation of DHA has been used to deep the mechanisms involved in **photocatalysis assisted by pressure and temperature**. Comparing to individual processes, we highlighted the formation of new products in particular hydroxyacetone (HydA) and acrylic acid (AcrAc) issue from the transformation of PA and LA. The greater the number of photons, the more PA and LA transformation and formation of new products. Transformation of PA and LA and formation of HydA and AcrAc are similar in presence of TiO_2 containing anatase phase but very low in presence of TiO_2 rutile. This behavior shows that acido /basicity of the TiO2 surface is not at the origin of the formation of these new products.We underscored that hydroxyacetone and acrylic acid come from the respective transformation of PA and LA.

It is also important to note the formation of H_2 and CO_2 in important concentration comparing to their detection in the both individual processes and the formation of acetaldehyde not observed with individual processes. Moreover, by using HPLC/MS, the formation of new condensation products, $C_6H_8O_3$ and $C_5H_6O_2$ are detected which could be explained by transformation of $C_6H_6O_3$ formed in the dark.

The formation of these new products obtained during the transformation of DHA under photocatalysis assisted by pressure and temperature highlights two types of reactions, dehydration and reduction reactions**.**

- **dehydration can be explained considering the generation of H^+** by photocatalysis, case of acrylic acid and $C_6H_8O_3$ formation

And

- **reduction reaction is explained by the availability of electrons** generated made possible thanks to oxidation reaction occurring via h^+ and or OH°. These oxidation reactions are improved either thanks to simultaneous generation and reaction of (e^-, h^+) and (H^+, OH^-) on TiO_2 surface due respectively to photocatalysis and protolysis or thanks to modification of electronic properties of TiO_2 under irradiation favoring adsorption of LA and subsequently oxidation. It is the case of the formation of hydroxyacetone.

The highlighting of the dehydration and reduction reactions under photocatalysis assisted by pressure and temperature needs to be deepened using other types of catalysts and other types of molecules to better understand the behavior of different functions under this type of process and develop products with high added value.

Acknowledgements

"This Special Issue is dedicated to honor the retirement of Prof. Santiago Esplugas at the Universitat de Barcelona (UB, Spain), a key figure in the area of Catalytic Advanced Oxidation Processes". The authors also acknowledge the « Centre Commun de Spectrométrie de Masse, ICBMS for its support.

References

[1] P. Sudarsanam, H. Li, T. Vikram Sagar, ACS Catal. 10 (2020) 9555–9584. doi-org.docelec.univ-lyon1.fr/10.1021/acscatal.0c01680

[2] A. G. Chakinala, J. K. Chinthaginjala, K. Seshan, W.P.M. van Swaaij, S. R.A. Kersten, D. W.F. Brilman, Catalysis Today 195 (2012) 83-92. dx.doi.org/10.1016/j.cattod.2012.07.042

[3] C. Li, J. Li, L. Qin, P. Yang, D. G. Vlachos, ACS Catal. 11 (2021) 11336–11359. dx.doi.org/10.1021/acscatal.1c02551

[4] L. Shiamala, K. Vignesh, B.M. Jaffar Al, Fuel 333 (2023) 126332. doi.org/10.1016/j.fuel.2022.126332

[5] C. W. J. Murnaghan, N. Skillen, B. Hackett, J. Lafferty, P. K. J. Robertson, G. N. Sheldrake, ACS Sustainable Chem. Eng. 10 (2022) 12107−12116. doi.org/10.1021/acssuschemeng.2c01606

[6] L. Llatance-Guevara, N.E.Flores, G.O. Barrionuevo, J.L. Mullo Casillas, Catalysts 12 (2022) 1091. doi.org/10.3390/ catal12101091

[7] G. C. de Assis, I. M. A. Silva, T. G. dos Santos, T. V. dos Santos, M. R. Meneghetti, S. M. P. Meneghetti, Catal. Sci. Technol., 11 (2021) 2354.doi-org.docelec.univ-lyon1.fr/10.1039/D0CY02358B

[8] J-C. Colmenares, R.Luque; Chem.Soc.Rev., 43 (2014) 765-778. DOI: 10.1039/C3CS60262A

[9] K. Czelej, J- C.Colmenares, K. Jabłczynska, K.Cwieka, L. Werner, L. Gradon, Catalysis Today 380 (2021) 156–186. doi.org/10.1016/j.cattod.2021.02.004

[10] S. Ning, S. Wang, S. Ouyang, Y. Qi, X. Yi, H. Hu, J. Ye, Catalysis Sciences and Technology, 11 (2021) 7029-7034. doi.org/10.1039/D1CY01435H

[11] S. Ning, Y.Sun, S.Ouyang, Y.Qi, J. Ye, Appl.Catal. B: Environ.310 (2022) 121063, doi.org/10.1016/j.apcatb.2022.121063

[12] C. Ren, X. Liu, G. Wang, S. Miao, Y. Chen, Thermo-photocatalytic degradation of benzene on Pt-loaded TiO2/ZrO2, J. Mol. Catal. Chem., 358 (2012) 31-37, https://doi: 10.1016/j.molcata.2012.02.007.

[13] Y. Li, J. Huang, T. Peng, J. Xu, X. Zhao, Photothermocatalytic Synergetic Effect Leads to High Efficient Detoxification of Benzene on TiO2 and Pt/TiO2 Nanocomposite, ChemCatChem, 2(9) (2010) 1082-1087, https:// doi: https://doi.org/10.1002/cctc.201000085.

[14] X. Yang, S. Liu, J. Li, J. Chen, Z. Rui, Chemosphere, 249 (2020) 126096, doi: 10.1016/j.chemosphere.2020.126096.

[15] W. Ji, Z. Rui, H. Ji, Ind. Eng. Chem. Res., 58 (31) (2019) 13950-13959, doi: 10.1021/acs.iecr.9b02176,

[16] W. Ji, T. Shen, J. Kong, Z. Rui, Y. Tong, , Ind. Eng. Chem. Res., 57(38) (2018) 12766-12773, doi: 10.1021/acs.iecr.8b02873

[17] F. Meng, Y. Liu, J. Wang, X. Tan, H. Sun, S. Liu, S. Wang, Journal of Colloid and Interface Science, 532 (2018) 321-330. doi.org/10.1016/j.jcis.2018.07.131

[18] M. Li, Y. Wang, Y. fan, L. Liao, X. Zhou, S. Mo, Y. Wang, Journal of Colloid and Interface Science, 608 (2022).3004-3012. doi.org/10.1016/j.jcis.2021.11.029

[19] G. Wang, B. Huang, Z. Lou, Z. Wang, X. Qin, X. Zhang, Y. Dai, Appl. Catal. B Environ. 180. (2016) 6–12. doi.org/10.1016/j.apcatb.2015.06.010

[20] N. Keller, J. Ivanez, J. Highfield, A. M. Ruppert, Appl. Catal. B: Environm.l 296 (2021) 120320. doi.org/10.1016/j.apcatb.2021.120320

[21] X. Han, M. Li, Y. Ma, Y. Li, H. Ma, et C. Wang, Surf. Interfaces, 23 (2021) 101006. doi: 10.1016/j.surfin.2021.101006.

[22] I. Rossetti, A. Villa, C. Pirola, L. Prati, et G. Ramis, RSC Adv. 4 (55) (2014) 28883-28885. doi: 10.1039/C4RA03751K

[23] I. Rossetti, A. Villa, M. Compagnoni, L. Prati, G. Ramis, C. Pirola, C.L.Bianchi, W. Wang, D. Wang, Catal. Sci. Technol. 5 (9) (2015) 4481-4487. doi: 10.1039/C5CY00756A.

[24] E. Bahadori, A. Tripodi, A. Villa, C. Pirola, L. Prati, G. Ramis, I. Rossetti, 8 (10) (2018) 430. doi:10.3390/catal8100430

[25] A. Nakatani, N. Kometani, Journal of Physics: Conference Series; 215 (2010) 012091. doi:10.1088/1742-6596/215/1/012091

[26] J. Zou, G. Zhang, et X. Xu, Appl. Catal. Gen. 563 (2018) 73-79, doi: 10.1016 / j.apcata. 2018.06.030

[27] I. Abdouli, F. Dappozze , M. Eternot , N. Essayem , C. Guillard, Appl. Catal. B: Environ. 305 (2022) 121051. doi.10.1016/j.apcatb.2021.121051

[28] I. Abdouli, F. Dappozze, M. Eternot, C. Guillard, N.Essayem, Molecules, 27 (2022) 8172. doi: 10.3390/molecules27238172

[29] E. Jolimaitre, D. Delcroix, N. Essayem, C. Pinel, M. Besson, Catal. Sci. Technol. 8 (2018) 1349–1356. doi.org/10.1039/C7CY02385E.

[30] E.M. Albuquerque, L.E.P.Borges, M.A.Fraga, C. Sievers, ChemCatChem. 9 (2017) 2675–2683. doi.org/10.1002/cctc.201700305.

[31] R. O. L. Souza, D. P. Fabiano, C. Feche, F. Rataboul, D. Cardoso, N. Essayem, Catal. Today, 195, (2012) 114-119, doi: 10.1016/j.cattod.2012.05.046.

[32] C. Moreau, J. Lecomte, A. Roux, Catal. Commun., 7 (2006) 941-944 doi: 10.1016/j.catcom.2006.04.001

[33] Y. Kim, A. Mittal, D. J. Robichaud, H. M. Pilath, B. D. Etz, P. C. St. John, D. K. Johnson, S. Kim, ACS Catal., 10 (2020) 14707-14721. doi: 10.1021/acscatal.0c04245.

[34] H.E. Krizner, D.O.Haan, J.Kua, J. Phys. Chem. 113 (2009) 6994-7001. Doi:10.1021/jp903213k.

[35] L. Elsellami, F. Vocanson, F. Dappozze, R. Baudot, G. Febvay, M. Rey, A. Houas, C. Guillard; Appl. Catal. B: Environ.,94 (2010) 192-199. doi.org/10.1016/j.apcatb.2009.11.009.

[36] A. V. Emeline, V. Ryabchuk, N. Serpone, J. Photochem. Photobiol. A : Chem., 133(2000) 89–97. doi:10.1016/s1010-6030(00)00225-2

[37] Y. Xu, C. H. Langford, J. Photochem. Photobiol. A: Chem., 133(2000), 67–71. doi:10.1016/s1010-6030(00)00220-3.

[38] A. Huyghues-Despointes, V. A. Yaylayan, J. Agric. Food Chem. 44 (1996) 672−681. doi.org/10.1021/jf9502921

[39] O. Novotný, K. CeJpeK, J. VelíšeK , Czech J. Food Sci., 25(3), (2007) 119–130. doi: 10.17221/740-CJFS.

[40] M.R.K. Estahbanati, A. Babin, M. Feilizadeh, Z.Nayernia, N. Mahinpey, M.C. Iliuta, Journal of Cleaner Production, 318(2021) 128546. doi.org/10.1016/j.jclepro.2021.128546